

# A new special function related to a discrete Gauss-Poisson distribution and some physics of the cell model with Curie-Weiss interactions

O. A. Dobush and M. A. Shpot

*Institute for Condensed Matter Physics, 79011 Lviv, Ukraine*

December 10, 2024

## Abstract

Inspired by previous studies in statistical physics [see, in particular, Kozitsky et al., *A phase transition in a Curie-Weiss system with binary interactions*, *Condens. Matter Phys.* **23**, 23502 (2020)] we introduce a discrete Gauss-Poisson probability distribution function

$$p_{GP}(n; z, r) = [R(r; z)]^{-1} \frac{e^{zn}}{n!} e^{-\frac{1}{2}rn^2} \quad (\text{A1})$$

with support on  $\mathbb{N}_0$  and parameters  $z \in \mathbb{R}$  and  $r \in \mathbb{R}_+$ . The probability mass function  $p_{GP}(n; z, r)$  is normalized by the special function  $R(r; z)$ , given by the infinite sum

$$R(r; z) = \sum_{n=0}^{\infty} \frac{e^{zn}}{n!} e^{-\frac{1}{2}rn^2}, \quad (\text{A2})$$

possessing extremely interesting mathematical properties. We present an asymptotic estimate  $R^{(\text{as})}(r; z \gg 1)$  for the function  $R(r; z)$  with large arguments  $z$ , along with similar formulas for its logarithm and logarithmic derivative. These functions exhibit very interesting oscillatory behavior around their asymptotics, for parameters  $r$  above some threshold value  $r^*$ . Some implications of our findings are discussed in the context of the Curie-Weiss cell model of simple fluids.

**Keywords.** Phase transition, fluid's cell model, Curie-Weiss interactions, discrete Gauss-Poisson distribution, special functions, asymptotic behavior

**2020 Mathematics Subject Classification.** Primary 33C20; Secondary 33C05

## 1 Introduction

Although a number of physical aspects of the cell model with binary Curie-Weiss interactions will be discussed in what follows, the main message of the present communication concerns the special function  $R(r; z)$  that normalizes the discrete Gauss-Poisson probability distribution function introduced in (A1). We shall come up with several useful physical conclusions throughout the paper. However, our primary goal is to bring the essentially unknown mathematical objects (A1) and (A2) arising in a specific branch of theoretical physics to the broad mathematical community. To the best of our knowledge, neither the discrete Gauss-Poisson probability

distribution function  $p_{GP}(n; z, r)$  nor the special function  $R(r; z)$  have been considered in the mathematical literature before.

The function  $R(r; z)$  seems to appear for the first time in the physical paper [1, p. 440] where the sum of exactly the same functional form as in (A2) resulted from certain integration and started with  $n = 2$ . In an even more general form, where the second power of the summation index  $n$  in (A2) is replaced by  $n^m$ , the sum appears in [2, p. 20]. In different disguises, the function  $R(r; z)$  can be found in a series of papers [3, p. 810, (3.15)], [4, p. 5, (2.15)], [5, p. 3, (17)], [6, p. 3, (9)], where the statistical mechanics calculations were based on grand canonical ensemble (see e.g. [7, Sec. 2.4]). Apparently, the functional form of the function  $R(r; z)$  in (A2) should be characteristic to calculations using this kind of statistics; actually, its general shape is the same as that of the grand-canonical partition function  $\Xi = \sum_{N=0}^{\infty} z^N Z_N/N!$  (see [7, (2.4.6)] and (5) below). Apart from the sum  $R(r; z)$  alone, for actual calculations of the mentioned papers several lowest-order moments

$$M_m(z, r) = [R(r; z)]^{-1} \sum_{n=0}^{\infty} n^m \frac{e^{zn}}{n!} e^{-\frac{1}{2}rn^2}, \quad m \in \mathbb{N} \quad (1)$$

of the distribution (A1) have been needed. However again, to the best of our knowledge, no mathematical properties of the sum  $R(r; z)$  or the moments  $M_m(z, r)$  have been studied in any physically oriented work, apart from their numerical evaluations using *truncated* series of exponentials.

The truncation of the series in (A2) or (1) is indeed an important dangerous aspect, which could potentially lead to negative consequences. The reason is that the asymptotic behavior of the finite series of the type (A2) as  $z \rightarrow +\infty$  qualitatively differs (at any order of truncation) from the true asymptotics of the infinite sum. We shall return to this issue in a subsequent publication.

Our motivation in the present work has several aspects.

(i) First of all, we are quite sure that it is of primary interest to initiate a mathematical investigation of the discrete Gauss-Poisson probability distribution function  $p_{GP}(n; z, r)$ , its normalization  $R(r; z)$ , and, further, the associated moments  $M(r; z)$ . In doing so, we have determined the non-trivial asymptotic behavior of  $R(r; z)$  along with some related functions and visualized an intriguing oscillating behavior of  $\ln R(r; z)$  in the vicinity of its asymptotics. Of course, it would be a highly interesting challenge to derive any explicit determinations of these functions for some special sets of parameters, although such a goal seems to be rather hopeless for the moment.

(ii) Certainly, it is expected that mathematical studies of this kind must have appropriate physical consequences and implications. An example is the issue of convergence of the master integral (7), involving  $\ln R(r; z)$  (see also (13)), in the marginal case of physical stability discussed in Sections 4 and 6. We hope that the list of such applications might be extended.

(iii) Our desire is to draw attention of mathematicians to the interesting and practically important mathematical objects discussed in the present communication and trigger their further investigation.

(iv) On the other side, we observed a lack of explicit analytical results in physical papers where the function  $R(r; z)$  and moments  $M_m(z, r)$  played an essential role, apart from a quite general proof [4] of the existence of phase transitions in underlying systems. All subsequent work, to be mentioned below, has been dedicated to numerical investigations. Here, we are starting to fill this gap, by presenting several instances of related analytical calculations and their implications.

## 2 Physical context

The special discrete Gauss-Poisson probability distribution function (A1) and associated infinite sums like (A2) and (1) appear in statistical mechanics investigations of simple classical fluids within the framework of the grand canonical ensemble. The physical basis for the present study is the cell model with binary Curie-Weiss interactions, introduced in [8, 4] for the purpose of modelling the simple fluids and describing phase transitions that occur in such physical systems. Extended studies of this model have been subsequently done in [9, 5], and, more recently in [6, 10].

In the following section, while describing the underlying physical model, we shall closely follow the reference [4].

### 2.1 Two-point interactions and their energy

It is assumed that a classical fluid system, which may be in a gaseous or liquid state, occupies a macroscopic container of volume  $V \subset \mathbb{R}^3$  in three space dimensions. The volume  $V$  is divided into  $N$  non-overlapping congruent cubic cells  $\Delta_\ell$  ( $\ell = 1, \dots, N$ ) of volume  $v = V/N$ . The system consists of a *variable* number  $n \in \mathbb{N}$  of point-like particles with three-dimensional coordinates  $\{x_1, \dots, x_n\}$ . The particles can randomly occupy any cell  $\Delta_\ell$  in the volume  $V$ .

The two-point interaction energy of particles with coordinates  $x_i$  and  $x_j$  is assumed to be

$$\Phi_N(x_i, x_j) = -\frac{J_1}{N} + J_2 \sum_{\ell=1}^N c_\ell(x_i) c_\ell(x_j). \quad (2)$$

Here:

- $J_1 > 0$  measures the strength of attraction between ANY two of  $n$  particles in  $V$
- $J_2 > 0$  is the strength of repulsion between the particles inside of a cell  $\Delta_\ell$
- $c_\ell(x_i)$  are the occupation indicators for the cell  $\Delta_\ell$ , they are defined via

$$c_\ell(x_i) = 1 \quad \text{if } x_i \in \Delta_\ell, \quad c_\ell(x_i) = 0 \quad \text{if } x_i \notin \Delta_\ell.$$

Thus, the overall energy of a system of  $n$  particles with the Curie-Weiss interactions in the volume  $V$  is given by

$$W_N^{(n)} = \frac{1}{2} \sum_{x_i, x_j} \Phi_N(x_i, x_j) = -\frac{1}{2} \frac{J_1}{N} n^2 + \frac{1}{2} J_2 \sum_{x_i, x_j} \sum_{\ell=1}^N c_\ell(x_i) c_\ell(x_j). \quad (3)$$

According to a rigorous result by Ruelle [11] (as quoted in [4]), the thermodynamic stability of the system under consideration is provided by the condition

$$\int_V dx \Phi_N(x, y) > 0 \quad \forall y \in V, \quad (4)$$

where the integrations runs over the three-dimensional volume  $V$  of the system, and we use a short-hand notation  $dx = d^3x$ . With  $\Phi_N(x, y)$  from (2), the condition (4) implies the requirement  $J_2/J_1 > 1$  [4, (2.3) – (2.4)]; see also (10).

All thermodynamic properties of the system derive from the grand-canonical partition function at the (absolute) temperature  $T$ ,

$$\Xi_N = \sum_{n=0}^{\infty} \frac{\zeta^n}{n!} Z_n, \quad Z_n = \int (dx)^n \exp[-\beta W_N^{(n)}], \quad (5)$$

where the inverse temperature  $\beta$  and activity (fugacity)  $\zeta$  are

$$\beta = \frac{1}{k_B T} \quad \text{and} \quad \zeta = \frac{e^{\beta \mu_{\text{phys}}}}{\Lambda^3}, \quad (6)$$

$k_B$  is the Boltzmann constant,  $\mu_{\text{phys}}$  is the physical chemical potential, and  $\Lambda$  is the de Broglie thermal wavelength. As in [4], we set  $\Lambda := 1$  in what follows.

## 2.2 The integral representation of grand-canonical partition function

An explicit calculation detailed in [4] yields a single-integral representation for the grand-canonical partition function  $\Xi_N$  of the cell model with Curie-Weiss interactions. Using a parametrization slightly differing from that accepted in [4], we reproduce it in the form

$$\Xi_N \equiv \Xi_N(p, r, \mu, v) = \sqrt{\frac{N}{2\pi p}} \int_{-\infty}^{\infty} dy e^{NE(p, r, \mu, v; y)}. \quad (7)$$

Here

$$E(p, r, \mu, v; y) = -\frac{y^2}{2p} + \ln K(p, r, \mu, v; y), \quad (8)$$

while

$$K(p, r, \mu, v; y) = \sum_{n \geq 0} \frac{v^n}{n!} e^{(y+p\mu)n - \frac{1}{2}rn^2} = R(r; y + p\mu + \ln v) \quad (9)$$

where we encounter just the function  $R(r; z)$  from (A2), with a shifted argument.

In the limit  $N \rightarrow \infty$ , we have  $\lim_{N \rightarrow \infty} \Xi_N = \exp[E(\dots; \bar{y})]$ , where  $E(\bar{y})$  is the maximum value of  $E(y)$  at the maximum point  $\bar{y}$ , which is defined as a solution to the extremum condition  $E'(y) = 0$ , provided that  $E''(\bar{y}) < 0$ . The limit  $N \rightarrow \infty$  employed in (7) for evaluation of this integral via the Laplace method is directly related to the thermodynamic limit, which is performed at fixed cell volume  $v$ . This drives the system's volume  $V$  to infinity, while  $v$  can be fixed at  $v = 1$  in subsequent calculations.

At this point it is important to stress the similarities and differences in variables and parameters employed in [4] and throughout the present paper.

The two independent fundamental thermodynamic variables in the problem are the inverse temperature  $\beta \geq 0$  and the physical chemical potential  $\mu_{\text{phys}} \in \mathbb{R}$ . As before, the dimensionless, normalized inverse temperature is defined as  $p = \beta J_1 \geq 0$ . Its counterpart, that involves the interaction parameter  $J_2$  in place of  $J_1$ , is  $r = \beta J_2 \geq 0$ . These variables are proportional one to another, and their ratio

$$\frac{r}{p} = J_2/J_1 \equiv a > 1 \quad \text{in notation of [4],} \quad \text{and} \quad \frac{r}{p} = J_2/J_1 \equiv f > 1 \quad \text{in notation of [5].} \quad (10)$$

Basically, *any one* of the quantities  $p$  and  $r$  can be chosen to represent the normalized inverse temperature. In [4], the role of such a variable has been assigned to  $p$ , and, consequently, the

remaining temperature-like quantity  $r$  had to be represented as  $r = p \frac{r}{p} = p a$ . The inequalities  $a = f > 0$  are a direct consequence of the thermodynamic stability condition (4).

Further, the dimensionless combination  $\beta\mu_{\text{phys}}$  appearing in the fugacity (6) is a product of two independent physical variables. Thus, accepting, similarly as in [4], that the quantity  $p$  represents the temperature, we write  $\beta\mu_{\text{phys}} = (\beta J_1) \cdot \mu_{\text{phys}}/J_1 \equiv p\mu$ , where we define the dimensionless, normalized chemical potential  $\mu \in \mathbb{R}$  via  $\mu \equiv \mu_{\text{phys}}/J_1$ .

We stress that our parametrization of physical variables related to the temperature ( $p = \beta J_1$ ) and chemical potential ( $\mu = \mu_{\text{phys}}/J_1$ ) differs from that accepted in [4]. In fact, there the inverse temperature  $\beta$  appears in the "basic set of thermodynamic variables" ( $p, \mu$ ) two times, both in  $p$  and in  $\mu$ , due to the definition of  $\mu = \beta\mu_{\text{phys}}$  (see [4, p. 3]), which combines two physically distinct and independent variables  $\beta$  and  $\mu_{\text{phys}}$  into one.

### 3 Some simple special cases

It seems that in the previous publications on the cell model described in Section 2.1 no simple limiting cases have been considered, such as the high-temperature limit  $\beta \rightarrow 0$  with finite interactions  $J_1, J_2 > 0$ , or the ideal gas with vanishing interactions  $J_1 = J_2 = 0$  at arbitrary temperature  $\beta$ . These special cases would require calculations of the grand partition function  $\Xi_N(p, r, \mu, v)$  in the limit of vanishing parameter  $p = \beta J_1$ . However, it is not evident how to proceed with this limit starting from the integral representation (7) with the function  $E$  given in (8) in the integrand.

To avoid the apparent difficulty with the  $p \rightarrow 0$  limit in (7), we slightly modify this integral by scaling the integration variable via  $y = t\sqrt{p}$ . Moreover, we find it helpful to use the explicit expressions for the normalized quantities  $p, r$  and  $\mu$  introduced in the previous section. Thus we write the integral representation (7) in the form

$$\Xi_N(J_1, J_2; \beta, \mu_{\text{phys}}; v) = \sqrt{\frac{N}{2\pi}} \int_{-\infty}^{\infty} dt \exp \left\{ N \left[ -\frac{t^2}{2} + \ln \sum_{n \geq 0} \frac{v^n}{n!} e^{(t\sqrt{\beta J_1} + \beta\mu_{\text{phys}})n - \frac{1}{2}\beta J_2 n^2} \right] \right\}. \quad (11)$$

Hence, in the case of a noninteracting ideal gas with  $J_1 = J_2 = 0$  and arbitrary finite  $\beta < \infty$  and  $\mu_{\text{phys}} < \infty$ , we remain with a simple summation in (11) and obtain the grand-canonical partition function  $\Xi_N(0, 0; \beta, \mu_{\text{phys}}; v)$  as

$$\Xi_N^{(id)}(\beta, \mu_{\text{phys}}, v) = \sqrt{\frac{N}{2\pi}} \int_{-\infty}^{\infty} dt \exp \left\{ N \left[ -\frac{t^2}{2} + \ln \sum_{n \geq 0} \frac{v^n}{n!} e^{\beta\mu_{\text{phys}}n} \right] \right\} = \exp(Nv e^{\beta\mu_{\text{phys}}}). \quad (12)$$

Thus,  $\ln \Xi_N^{(id)}(\beta, \mu_{\text{phys}}, v) = V e^{\beta\mu_{\text{phys}}}$  in agreement (up to the factor  $\Lambda^{-3}$ , see (6)) with the well-known classical result, which can be found, for example, in [12, p. 395, (A2.11)].

The high-temperature limit  $\beta = 0$  becomes trivial:

$$\ln \Xi_N(J_1, J_2; 0, \mu_{\text{phys}}; v) = \ln \Xi_N^{(id)}(0, \mu_{\text{phys}}, v) = V e^{\beta\mu_{\text{phys}}} \Big|_{\beta=0} = V.$$

The special case  $J_1 = J_2 = 0$  is interesting in view of the thermodynamic stability requirement (4) as the latter implies the inequality  $f = J_2/J_1 > 1$  (see (4), (10)). When  $J_1 = J_2 = 0$ , we have to do with the extreme limit of the equality case  $J_1 = J_2$  corresponding to the stability edge given by  $f = 1$ . The existence of this limit is not anticipated by the condition (4), but,

nevertheless, we just obtained a sensible and expected result in this marginal case. This observation suggests that it would be of interest to consider the special case of equal non-vanishing attraction and repulsion interactions  $J_1 = J_2 > 0$  in (2), that is  $f = 1$  and  $0 < r = p < \infty$  (see Sec. 2.2 around the equation (10)).

Another limiting case of strong repulsion interactions within the cells,  $J_2 \rightarrow \infty$ , with arbitrary and independent strength of attraction between particles  $J_1 > 0$  will be considered separately in Sec. 7.

And now, we shall turn to a consideration of the convergence of equivalent basic integrals, (7) or (11), on the edge of the thermodynamic stability,  $J_1 = J_2$ .

## 4 The issue of convergence of the integral (11) at the edge of stability

Having solved the problem related to the special case  $p = 0$  in the preceding section, for finite parameters  $0 < p < \infty$  we can safely return to the integral representation (7). Here, following [5], we shift the integration variable via  $y = z - \mu - \ln v$ . Thus our starting point will be now the integral

$$\Xi_N(p, r, \mu, v) = \sqrt{\frac{N}{2\pi p}} \int_{-\infty}^{\infty} dz \exp \left\{ N \left[ -\frac{1}{2p} (z - p\mu - \ln v)^2 + \ln R(r; z) \right] \right\}, \quad (13)$$

where the function  $R(z; r)$  appears as it is announced in (A2). In comparison to (7), in the present representation (13), the sum  $R(r; z)$  under the logarithm contains *only one* physical parameter, namely the temperature-like thermodynamic variable  $r = \beta J_2$ . All remaining "physics" enters the first simple quadratic term.

Completing the square in the exponent of the exponential in the summands of (18), we have

$$zn - \frac{1}{2} rn^2 = \frac{z^2}{2r} - \frac{r}{2} \left( n - \frac{z}{r} \right)^2, \quad (14)$$

where the first term on the right-hand side is the maximal value of the quadratic form on the left, for any  $n \geq 0$ . Hence, for the grand-canonical partition function  $\Xi_N$  in (13) we can write

$$\Xi_N \propto e^{-\frac{N}{2p} (p\mu + \ln v)^2} \int_{-\infty}^{\infty} dz \exp \left\{ N \left[ -\frac{z^2}{2p} (1 - b) + (\mu + p^{-1} \ln v) z + \ln \hat{R}(r; z) \right] \right\}, \quad (15)$$

where we defined the ratio  $b := \frac{p}{r} = \frac{J_1}{J_2}$  in the range  $b \in [0, 1]$  (cf. (10)) and the modified  $R$ -sum (cf. (18))

$$\hat{R}(r; z) := \sum_{n \geq 0} e^{-\frac{r}{2} \left( n - \frac{z}{r} \right)^2}. \quad (16)$$

Here we observe that the procedure of completing the square in (14) shows up the value of the greatest summand in (18), namely  $e^{\frac{z^2}{2r}}$ , which thus defines the leading term of the asymptotic behavior of the sum  $R(r; z)$  for large  $z$  (cf. (21)). To determine further, sub-leading terms of the asymptotic expansion of  $R(r; z)$  one would have to employ more elaborated techniques as described in [13, 14, 15, 16].

And, for moment, we just notice that while the function  $\ln R(r; z)$  roughly behaves as

$$\ln R(r; z) \sim \frac{z^2}{2r} + o(z^2) \quad \text{when} \quad z \rightarrow \infty, \quad (17)$$

this implies that the function  $\ln \hat{R}(r; z) \sim o(z^2)$  as  $z \rightarrow \infty$ . Thus, for the integral (15) this means, that its convergence at large  $z$  is controlled by the first quadratic term  $\propto -z^2(1-b)$  for all  $b$  but  $b=0$  when this term simply disappears. In particular,

- the inequality  $b < 1$  ensures the convergence of the integral over  $z$  in (15), in agreement with (4) and (10);
- with  $b > 1$  the integral would diverge, which corresponds to an unphysical situation;
- the marginal case  $b = 1$  requires a special consideration taking into account the asymptotic behavior of the function  $\ln \hat{R}(r; z)$

In fact, in the absence of the leading  $\propto z^2$  term in (15), the convergence of the integral at large  $z$  is controlled by the leading term of the asymptotics of  $\ln \hat{R}(r; z)$ , that is, by the sub-leading term in the asymptotic expansion of the function  $\ln R(r; z)$  denoted by  $o(z^2)$  in (17).

In the following sections we shall present asymptotic estimates  $R^{(\text{as})}(r; z \gg 1)$  for the function  $R(r; z)$  at large arguments  $z$  and find an answer to the question of convergence of the integral representation (13) for the grand-canonical partition function  $\Xi_N(p, r, \mu, \nu)$  in the marginal case  $r = p$ , that is  $b = 1$  in (15).

## 5 The function $R(r; z)$ and its asymptotics

The function

$$R(r; z) = \sum_{n \geq 0} \frac{e^{zn}}{n!} e^{-\frac{1}{2}rn^2} \quad (18)$$

is well defined for any  $r \geq 0$  and  $z \in \mathbb{R}$ .

At  $r = 0$ , the exact result of the summation in (18) is  $R(0; z) = \exp(e^z)$ , while in the limit  $r \rightarrow \infty$  only the first term of the sum survives and thus we have  $R(\infty; z) = 1$ . Hence, for any  $0 \leq r < \infty$ , the function  $R(r; z)$  lies within the bounds  $1 \leq R(r; z) < \exp(e^z)$  and therefore  $0 < \ln R(r; z) < e^z$ . Moreover, for  $r > 0$ , the estimate from above  $R(r; z) \leq e^{z^2/(2r)+1}$  has been used in [4].

In the following, we shall be interested the asymptotic behavior of the function  $R(r; z)$  for finite  $0 < r < \infty$  and  $z \gg 1$ .

### 5.1 The asymptotic behavior of $R(r; z)$

In order to obtain an asymptotic evaluation of the sum (18) in the limit  $z \rightarrow \infty$  we employed a discrete analogue of the Laplace method (see e.g. [13, 17, 14, 18, 19, 15, 20, 21]) commonly used for asymptotic approximations of integrals.

By contrast to the case of the asymptotic analysis of integrals, the literature on its discrete version for sums is very scarce. The discrete Laplace method is telegraphically outlined in the well-known books by de Bruijn [13, Ch. 3], Bender and Orszag [14, p. 304 – 305], and Flajolet and Sedgewick [15, p. 761 – 762]. A detailed development of the discrete Laplace method capable of producing the next-to-leading terms of the asymptotic expansion has been performed in the paper by Paris [16], where several additional relevant references can also be

found. However, its exposition is based on a rather specific example and seemingly does not provide any explicit receipt for treating the asymptotic behavior of generic discrete sums.

For the sum (18) we have found the asymptotic formula

$$R^{(\text{as})}(r; z \gg 1) \sim \frac{e^{-\frac{r}{2}q^2}}{\sqrt{1+rq}} \left( \frac{e^{z+1}}{q} \right)^q, \quad \text{where} \quad q = \frac{1}{r} W(re^z), \quad (19)$$

and  $W(x)$  is the Lambert  $W$ -function, the solution to the equation  $We^W = x$ . An exiting introduction to the Lambert  $W$ -function can be found in the excellent paper [22].

The asymptotic formula (19) holds for arbitrary finite  $r \in \mathbb{R}_+$ , *including*  $r = 0$ , in which case it reproduces the exact result  $R(0; z) = \exp(e^z)$  valid for any  $z < \infty$ . This can be easily checked by using the Taylor expansion of the Lambert  $W$ -function  $W(x \rightarrow 0) = x + O(x^2)$  [22, (3.1)].

Shifting the summation index in  $R(r; z)$  and using (19) we derived the asymptotic estimate for the function  $R_1(r; z) \equiv \frac{d}{dz}R(r; z)$ :

$$R_1^{(\text{as})}(r; z \gg 1) \sim \frac{e^{-\frac{r}{2}q_1^2}}{\sqrt{1+rq_1}} \left( \frac{e^{z+1-r}}{q_1} \right)^{q_1} \cdot e^{z-r/2} \quad \text{with} \quad q_1 = \frac{1}{r} W(re^{z-r}). \quad (20)$$

Again, the exact result  $R_1(0; z) = \exp(e^z)e^z$  is reproduced from the last equation.

The asymptotic formula (19) can be simplified to the form involving only elementary functions. The result is, with the notation  $\zeta \equiv z/r$ ,

$$r \ln R^{(\text{as})}(r > 0; z \gg 1) \sim \frac{1}{2} z^2 - z(\ln \zeta - 1) + \frac{1}{2} \ln^2 \zeta - \frac{r}{2} \ln z + O\left(\frac{\ln \zeta}{z}\right). \quad (21)$$

As we see, the asymptotic expansion (21) includes all divergent terms along with a constant, while all descending terms are discarded. It is also observed that the leading term of the asymptotic expansion of the function  $r \ln R(r; z)$  does not depend on  $r$ .

Furthermore, the evaluation (21) implies, for finite  $0 < r < \infty$ ,

$$r \frac{d \ln R(r; z)}{dz} = r \frac{R_1(r; z)}{R(r; z)} \sim z - \ln \zeta + \frac{1}{2z} (2 \ln \zeta - r) + O\left(\frac{\ln \zeta}{z^2}\right), \quad z \gg 1. \quad (22)$$

The information of this kind can be interesting in the context of studying the moments (1) of the discrete Gauss-Poisson probability distribution function (A1).

In deriving the simplified asymptotics (21), we employed the asymptotic expansion of the Lambert function  $W(e^z)$  at  $z \rightarrow \infty$  (cf. [22, (4.19)]):

$$W(e^z) \sim z - \ln z + \frac{\ln z}{z} + O(z^{-2} \ln^2 z). \quad (23)$$

Since we used this expansion for the function  $qr = W(re^z)$  from (19) at large argument  $re^z$ , the alternative limit  $r \rightarrow 0$  has been lost in the results (21) and (22).

## 5.2 Graphical illustrations

In the present section, we show a few plots related to the function  $R(r; z)$  and its asymptotic behavior.



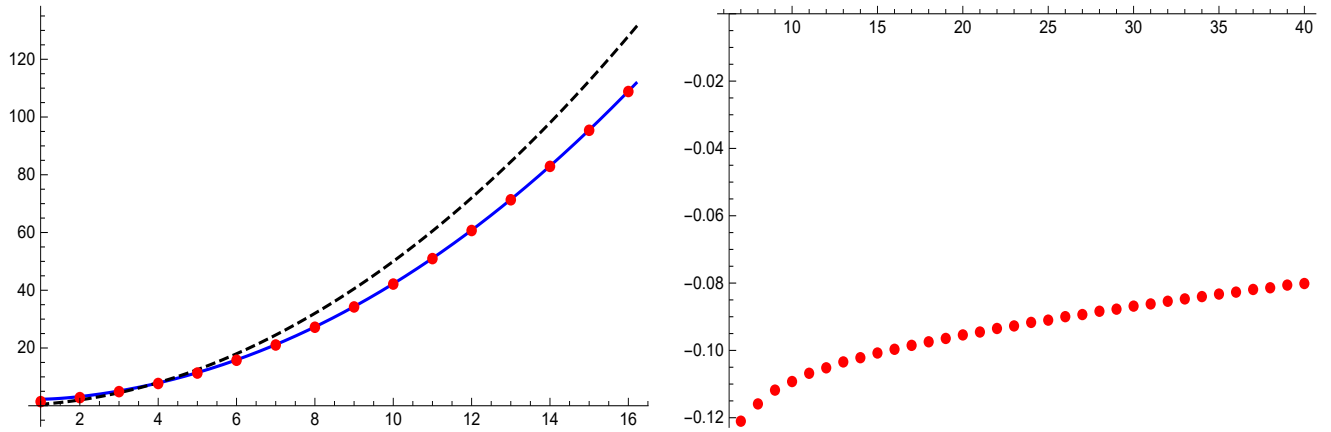


Fig 1. LEFT: Red dots: the function  $r \ln R(r; z)$  at  $r = 1.8$  and  $z = 1, \dots, 16$ . The solid blue line represents the asymptotics  $r \ln R^{(\text{as})}(r; z \gg 1)$  of the same function given by the formula (21). The dashed black line shows the leading asymptotic term  $z^2/2$  of  $r \ln R^{(\text{as})}(r; z \gg 1)$  from (21). RIGHT: The difference (24) between the function  $r \ln R(r; z)$  and its asymptotics from (21) at  $r = 1.8$ .

Figure 1 represents a comparison of the numerical calculation of the function  $r \ln R(r; z)$  (performed with the help of Mathematica [23]) and the analytical formula (21) for its asymptotics at  $r = 1.8$ . As we see, the asymptotic evaluation (21) compares very well with the full function  $r \ln R(r; z)$ . Moreover, as it often happens in the asymptotic analysis, the asymptotic formula derived under condition  $z \rightarrow \infty$  gives a good approximation for the underlying function even for rather small arguments  $z$ , like  $z = 2$  or  $3$ , which do not actually meet this requirement. The leading asymptotic term  $z^2/2$ , accessible in an elementary way by completing the square in exponents of summands in  $R(r; z)$  (see (14)) does not provide such a good fit as the formula (21).

In the above example we have taken a rather small value of the parameter  $r$ . In such a case, deviations of the original function  $r \ln R(r; z)$  from its asymptotics are very small, and their difference

$$r \ln R(r; z) - r \ln R^{(\text{as})}(r; z \gg 1) \quad (24)$$

shows a smooth monotonic behavior.

The situation changes drastically when we move towards larger values of the parameter  $r$  and exceed certain threshold value  $r = r^*$ . If we consider such  $r > r^*$ , the deviations between the function  $r \ln R(r; z)$  and its asymptotics become much more essential, and their difference (24) becomes oscillatory. Such situation is illustrated by the couple of graphs in Figure 2.

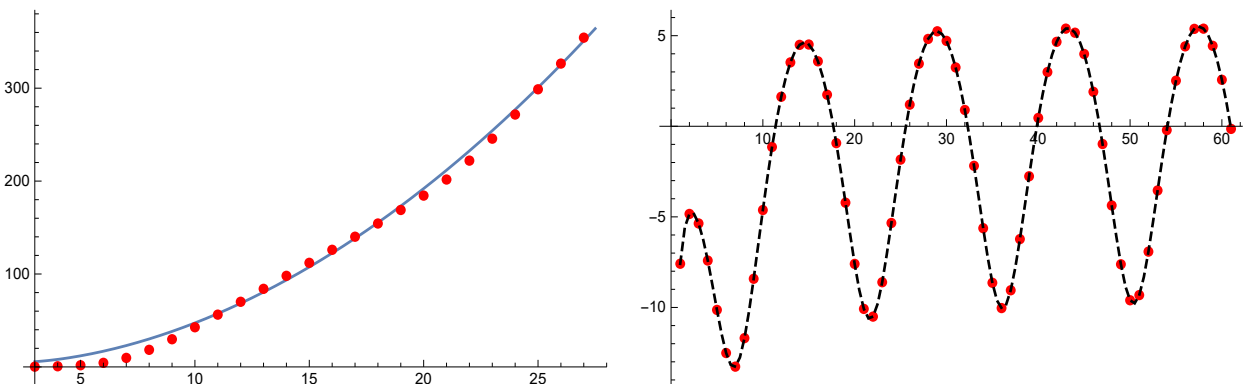


Fig 2. LEFT: Red dots: the function  $r \ln R(r; z)$  at  $r = 14$  and  $z = 3, \dots, 27$ . The solid blue line represents the asymptotics  $r \ln R^{(\text{as})}(r; z \gg 1)$  of this function given by the formula (21). RIGHT: Red dots: The difference (24) between the function  $r \ln R(r; z)$  and its asymptotics from (21). The dashed curve provides an eye-guide. The argument  $z$  is extended here up to  $z = 61$ .

Certainly, the functions  $R(r; z)$  and  $r \ln R(r; z)$ , and their non-trivial behavior in the vicinity of asymptotics deserve further investigation. Nevertheless, at the moment we return to the convergence issue raised in Sec. 4.

## 6 Back to the integral (13) at the stability edge

In Sec. 4, we have seen that the convergence of the integral (13), and thus, the stability of the underlying physical system, strongly depend on the value of the parameter  $b := \frac{p}{r} = \frac{J_1}{J_2}$  introduced in (15). While it was evident that in (15), the integral over  $z$  converges if  $b < 1$  and diverges if  $b > 1$ , the question of its behavior in the marginal case  $b = 1$  remained open. Now, possessing the required information on the large- $z$  behavior of its integrand, we are in a position to give a solution to this problem.

Let us write the integral over  $z$  in (15) as

$$\int_{-\infty}^{\infty} dz e^{N E(p, r; z)} \quad \text{with} \quad E(p, r; z) = -\frac{z^2}{2p} (1 - b) + (\mu + p^{-1} \ln v) z + \ln \hat{R}(r; z), \quad (25)$$

and the function  $\hat{R}(r; z)$  defined in (16). At  $b = 1$ , the quadratic term in  $E(p, r; z)$  disappears, and we set  $r = p$ . Thus we remain with the integrand

$$E(p, p; z) = (\mu + p^{-1} \ln v) z + \ln \hat{R}(p; z). \quad (26)$$

By the definition of the function  $\hat{R}(r; z)$  (see (14), (16)), the asymptotic behavior of  $\ln \hat{R}(p; z)$  at large argument  $z$  is given by

$$\ln \hat{R}(p; z \gg 1) = \ln R(p; z \gg 1) - \frac{z^2}{2p} \sim -\frac{z}{p} (\ln z - \ln p - 1) + O(\ln^2 z), \quad (27)$$

where the expression on the right-hand side results from the truncated asymptotic estimate (21) with the replacement  $r \mapsto p$ . Thus, for large enough  $z$  we have

$$E(p, p; z \gg 1) \sim -\frac{z}{p} \ln z + \frac{z}{p} (p \mu + \ln v + \ln p + 1) + O(\ln^2 z). \quad (28)$$

We see that the negative next-to leading asymptotic term  $\sim -z \ln z$  of the function  $p \ln R(p; z \gg 1)$  guarantees the convergence of the integral (25) at  $z \rightarrow +\infty$ .

This means that in the special case  $J_1 = J_2$  of (2), the mathematical problem to solve does not encounter any convergence problem, and thus can lead to meaningful results from a physical point of view. Its numerical solution may go along the lines of [4, 9], and [5], where only strictly smaller than unity values of  $b$  have been taken into account: See, for example, [4, Table 1], [9, p. 249] where a close-to-the-edge value  $a = b^{-1} = 1.0001$  has been considered among the others.

## 6.1 Explicit solution of the $b = 1$ problem in the asymptotic limit

Now, we are in a position to evaluate the integral (25) in the asymptotic limit, that is with the function  $E(p, p; z \gg 1)$  from (28) in the integrand. Let us write this function in the form  $E(p, p; z \gg 1) = p^{-1}(\hat{\mu}z - z \ln z)$  with the short-hand notation  $\hat{\mu} \equiv p\mu + \ln v + \ln p + 1$ .

As described after the equation (9), we have the extremum condition

$$E'_0(p, p; z \gg 1) = p^{-1}(\hat{\mu} - 1 - \ln z) = 0.$$

For finite  $p > 0$ , hence follows  $\ln \bar{z} = \hat{\mu} - 1$ , and  $\bar{z} = e^{\hat{\mu}-1}$  for the extremum position. The second derivative  $E''_0(p, p; z \gg 1) = -1/(pz) < 0$  as it should be within the Laplace method, indicating that the argument  $z = \bar{z}$  indeed corresponds to a maximum. The maximum's height is then

$$E(p, p; \bar{z} \gg 1) = p^{-1}[\hat{\mu}e^{\hat{\mu}-1} - e^{\hat{\mu}-1}(\hat{\mu} - 1)] = p^{-1}e^{\hat{\mu}-1} = p^{-1}e^{p\mu + \ln v + \ln p} = v e^{p\mu} = v e^{\beta\mu_{\text{phys}}},$$

which evaluates the integral in (25) and completely agrees with the ideal-gas result derived in the special case  $r = p = 0$  before, see (12).

It would be interesting to see whether the inclusion of more terms of the asymptotic expansion for the function  $E(p, p; z \gg 1)$  or employing the numerical analysis along the lines of [5] will produce deviations from the ideal-gas result obtained for the marginal case  $b = 1$  just above.

## 7 The strong-repulsion limit $J_2 \gg J_1$

In this section, we shall consider the limiting case of strong repulsion interactions within the cells, that is  $J_2 \rightarrow \infty$ , with arbitrary finite strength of attraction between particles  $J_1 > 0$  (see Sec. 2.1).

Our starting point will be the integral representation (7)-(9) where the large repulsion parameter  $J_2$  implicitly appears through the quantity  $r = \beta J_2$ . Following [4], we shall control the temperature using the dimensionless variable  $p$ , and for the parameter  $r$  we write  $r = (\beta J_1)J_2/J_1 = pf$  (cf. (10)). For our present purposes, the relation  $J_2 \gg J_1$  will be controlled by the ratio  $f \equiv J_2/J_1 \gg 1$ . With this in mind, we approximate the function  $K(p, r, \mu, v; y)$  in (9) via

$$K(p, r, \mu, v; y) \simeq \sum_{n=0}^1 \frac{v^n}{n!} e^{(y+p\mu)n - \frac{1}{2}rn^2} = 1 + v e^{y+p\mu - \frac{1}{2}pf} + O(e^{-2pf}), \quad (29)$$

that is, we take into account only the first non-trivial term in the sum (9). Without this exponential contribution, we would obtain a quite trivial result for the limit  $f = \infty$ .

Thus, we are going to consider the grand-canonical partition function  $\Xi_N(p, f \gg 1, \mu, v := 1)$  given by the integral (cf. (7)-(9))

$$\int_{-\infty}^{\infty} dy e^{N E(y)} \quad \text{with} \quad E(y) = \ln \left( 1 + e^{y+p\mu - \frac{1}{2}pf} \right) - \frac{y^2}{2p}. \quad (30)$$

### 7.1 A simple way to the critical point

To simplify the following expressions, we introduce short-hand notations

$$y + p\mu - \frac{1}{2}pf \equiv u(y) \quad \text{and} \quad e^{u(y)} \equiv x > 0. \quad (31)$$

It is conceivable that there is a special point  $y = y_0 = p(\frac{1}{2}f - \mu)$ , for which  $u(y_0) = 0$  and  $e^{u(y_0)} \equiv x_0 = 1$ .

To begin with, let us calculate the first derivative of the function  $E(y)$  from (30):

$$E'(y) = \frac{e^{u(y)}}{1 + e^{u(y)}} - \frac{y}{p} = \frac{px - y - yx}{p(1 + x)}. \quad (32)$$

Note that by the definition of the function  $x$  in (31), we have  $\frac{dx}{dy} = \frac{de^{u(y)}}{dy} = e^{u(y)} = x$ .

At the special point  $y = y_0$ , with  $x_0 = 1$  in (32), we have

$$E'(y_0) = \frac{p - 2y_0}{2p}, \quad (33)$$

and  $E'(y_0)$  vanishes when  $y_0 = \bar{y}_0 = p/2$ . By the definition of  $y_0$  as  $y_0 = \frac{p}{2}(f - 2\mu)$ , the extremum condition  $\bar{y}_0 = p/2$  implies the relation

$$\mu = \mu_c = \frac{1}{2}(f - 1) \quad (34)$$

between the underlying physical parameters of the problem.

According to the rules for calculating the integral over  $y$  in (30) using the Laplace method for large  $N$  given in page 4, we have to check the sign of the second derivative  $E''(y)$  at the extremum point  $y = \bar{y}_0$ . This second derivative has to be negative to provide that the function  $E(y)$  has a *maximum* at  $y = \bar{y}_0$ .

A straightforward calculation yields for the second derivative of  $E(y)$

$$E''(y) = \frac{e^{u(y)}}{(1 + e^{u(y)})^2} - \frac{1}{p} = -\frac{x^2 + (2 - p)x + 1}{p(1 + x)^2}. \quad (35)$$

In our special situation with  $y = y_0$ , we have

$$E''(y_0) = \frac{p - 4}{4p}. \quad (36)$$

This means that  $E''(y_0) < 0$  for any  $y_0$  if  $p < p_c = 4$ , including the extremum point found at  $y_0 = \bar{y}_0 = p/2$ , which thus appears to be a simple maximum. And, at the critical value of  $p$ ,  $p = p_c = 4$ , the second derivative  $E''(y_0)$  vanishes, thus indicating some more complicated behavior of the function  $E(y)$ .

To see the fate of the maximum  $E(\bar{y}_0)$  at  $p = p_c$ , we have to calculate the third and the fourth derivatives of  $E(y)$ . These are

$$E'''(y) = \frac{x(1 - x)}{(1 + x)^3} \quad \text{and} \quad E^{iv}(y) = x \frac{(1 - x)^2 - 2x}{(1 + x)^4}, \quad (37)$$

and it is noticeable that these higher derivatives have no explicit dependence on  $p$  and  $y$  in contrast to  $E'(y)$  and  $E''(y)$  in (32) and (35). With  $x = x_0 = 1$ ,

$$E'''(y_0) = 0 \quad \text{and} \quad E^{iv}(y) = -\frac{1}{8}. \quad (38)$$

This means that at  $p = p_c = 4$ , the simple maximum at  $\bar{y}_0 = p/2$  and  $p < 4$  transforms into a flat degenerate maximum at  $y_c = 2$  of the function

$$E_c(y) = \ln(1 + e^{y-2}) - \frac{y^2}{8}. \quad (39)$$

The maximum value of this function is  $E_c(y_c) = E_c(2) = \ln 2 - 1/2$ , which is a special case of (43) at  $p = 4$ .

Apart from the basic extremum condition  $E'(y) = 0$ , the conditions  $E''(y) = 0$  and  $E'''(y) = 0$  required at the critical point, are simplified analogs of equations [5, (28)] used in this reference for numerical determination of critical points of the underlying physical system.

We also observe that the equation  $E'''(y) = 0$  with  $E'''(y)$  given in (37) immediately yields the non-trivial solution  $x_0 = 1$ , and thus  $u(y_0) = 0$  chosen by inspection at the very beginning of the present section.

In our present setting with  $f \gg 1$ , we have found a critical point occurring at the (inverse) critical temperature  $p = p_c = 4$  and the critical value of the chemical potential  $\mu = \mu_c = \frac{1}{2}(f - 1)$ . The value  $p_c = 4$  agrees with that found numerically in [4, p. 13, Table 1] for  $f = a = 10$ . With this value of the parameter  $f$ , our calculation leads to the value  $\mu_c(10) = 9/2$ , while there is no information on its counterpart in [4]. The critical value  $p_c = 4$  agrees also with that found in [9, p. 249] for  $a = 10$ , while some discrepancy exists in evaluations of  $\mu_c$ . Our value  $\mu_c(10) = 9/2$  must be multiplied by  $p_c = 4$  to fit the notation  $\mu_c$  accepted in [9] (see p. 4). This would lead to  $\mu_c^{10} = 18$  in notation of [9], while the numerical result of this reference is  $\mu_c^{10} \simeq 15.5$ , the value of the same order of magnitude, but not quite the same; the difference being about 14%.

## 7.2 Temperature dependence of $E(y)$ at $\mu = \mu_c$

At the critical value of the chemical potential,  $\mu = \mu_c = (f - 1)/2$  (see (34)), the function  $E(y)$  from (30) reduces to

$$E(\mu_c; y) = \ln(1 + e^{y-p/2}) - \frac{y^2}{2p}. \quad (40)$$

The dependence on the large parameter  $f$  has disappeared, and the sole remaining physical parameter in (40) is the inverse temperature  $p$ . Different shapes of the function  $E(\mu_c; y)$  at different values of the parameter  $p$ , namely  $p < p_c$ ,  $p = p_c$ , and  $p > p_c$ , are shown in Fig. 3:

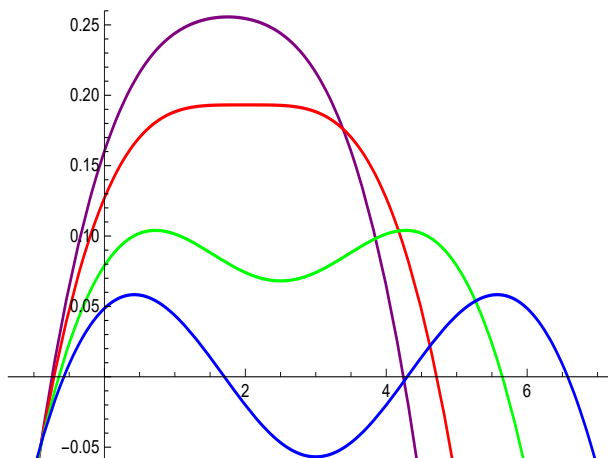


Fig. 3. Plots of the function  $E(\mu_c; y)$  from (40) at four different values of the parameter  $p$ :  $p = 3.5 < p_c$  (purple),  $p = 4 = p_c$  (red),  $p = 5 > p_c$  (green), and  $p = 6$  (blue). One can see that the purple maximum occurs at  $\bar{y}_3 = 1.75$ , the red one — at  $\bar{y}_4 = 2$ , and the green and blue minima — at  $\bar{y}_5 = 2.5$  and  $\bar{y}_6 = 3$ , respectively. Moreover, all curves are symmetric with respect to their extremum positions  $\bar{y}_p$ . The blue curve with  $p = 6$  is a counterpart of the blue one in Figure 4 of [4, p. 14].

The plot of  $E(\mu_c; y)$  at  $p = 6$  is analogous to that given in [4, p. 14, Fig. 4], and the both

are very similar even in numerical values, though the latter one is produced with the infinite sum over  $n$  in (29), and a different value of  $\mu_c$ .

Vanishing of the first derivative of  $E(\mu_c; y)$  given by (32) with  $u(y) = y - p/2$  yields the extremum condition

$$e^{y-p/2} = \frac{y}{p-y}. \quad (41)$$

An evident trivial solution to the last equation is  $\bar{y}_0 = p/2$ , the same as that following from (33). As far as  $p < p_c = 4$ , the coordinates  $\bar{y}_0 = p/2$  are the positions of simple maxima of  $E(\mu_c; y)$  represented by the purple line in Fig. 3. At  $p = p_c = 4$ , the maximum becomes degenerate and acquires the flat form presented by the red line in this figure. Further, when we move to  $p > p_c > 4$ , the extremum at  $\bar{y}_0 = p/2$  becomes a *minimum*. Two side maxima of equal height appear at the same time, and this situation is illustrated by the green and blue curves. The positions of these maxima are defined by two further solutions  $\bar{y}_1$  and  $\bar{y}_2$  to the extremum equation (41), apart of  $\bar{y}_0 = p/2$ .

To confirm the apparent symmetry of the curves in Fig. 3, we shift in  $E(\mu_c; y)$  the variable  $y$  via  $y - p/2 = s$ . Thus we obtain the function

$$\hat{E}(\mu_c; s) = \ln(1 + e^s) - \frac{1}{2p} \left( s + \frac{p}{2} \right)^2, \quad (42)$$

which becomes symmetric with respect to the ordinate. To see that  $\hat{E}(\mu_c; s)$  indeed is an even function, let us change  $s \mapsto -s$  in (42). Thus we obtain

$$\begin{aligned} \hat{E}(\mu_c; -s) &= \ln(1 + e^{-s}) - \frac{1}{2p} \left( -s + \frac{p}{2} \right)^2 = \ln[e^{-s}(1 + e^s)] - \frac{1}{2p} \left( s - \frac{p}{2} \right)^2 = \\ &= \ln(1 + e^s) - \frac{1}{2p} \left[ \left( s - \frac{p}{2} \right)^2 + 2ps \right] = \ln(1 + e^s) - \frac{1}{2p} \left( s + \frac{p}{2} \right)^2 = \hat{E}(\mu_c; s). \end{aligned}$$

In Fig. 4 we plot the function  $\hat{E}(\mu_c; s)$  in the same four cases as in Fig. 3. The whole picture becomes symmetric with respect to the axis  $s = 0$ .

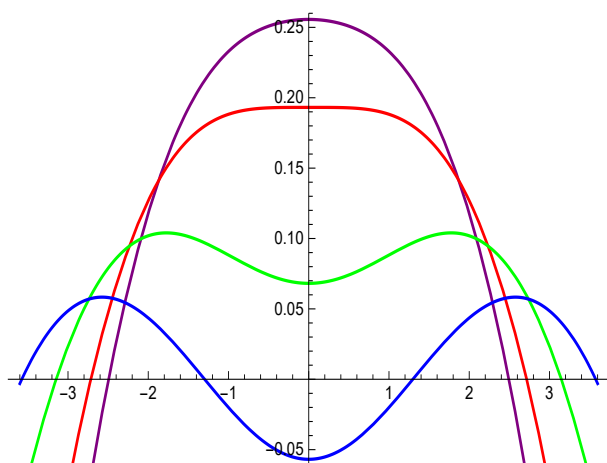


Fig. 4. Plots of the function  $\hat{E}(\mu_c; s)$  from (42) at the same values of  $p$  as in Fig. 3. All curves are symmetric with respect to the  $s = 0$  axis as it should be for the even function  $\hat{E}(\mu_c; s)$ .

The extremum positions of the function  $E(\mu_c; y)$  at  $\bar{y}_0 = p/2$  seen in Fig. 3 are mapped to a single point  $s = 0$  in Fig. 4. The heights of these extrema are given by

$$\hat{E}(\mu_c; 0) = \ln 2 - \frac{p}{8}. \quad (43)$$

Now, it becomes interesting to expand the function  $\hat{E}(\mu_c; s)$  in powers of its argument  $s$  around the origin. This yields

$$\hat{E}(\mu_c; s) \simeq \hat{E}(\mu_c; 0) + \frac{p-4}{8p} s^2 - \frac{s^4}{192} + O(s^6) \quad (44)$$

with the constant term  $E(\mu_c; 0)$  given in (43).

The functional form appearing in (44) precisely coincides with that of the usual Landau expansion with the critical value  $p_c = 4$  of the temperature parameter  $p$ , at which the  $O(s^2)$  term changes its sign, while the stability of the underlying physical system is guaranteed by the correct sign of the  $s^4$  term. This actually implies that in the strong-repulsion limit  $J_2 \gg J_1$  and the critical value of the chemical potential  $\mu_c$ , the Curie-Weiss model defined in Section 2.1 belongs to the wide universality class given by the Landau expansion (44). The closest in spirit representatives of this universality class are the lattice gas and other Ising-like systems in zero external field.

In the following section, we shall consider the behavior of the basic function  $E(y)$  from (30) for chemical potentials  $\mu$  differing from their critical value  $\mu_c$ .

### 7.3 Temperature dependence of $E(y)$ with $\mu \neq \mu_c$

In the present section, we are going to consider a quite generic situation where we relax the conditions  $u(y) = 0$  (see (31)),  $E'''(y) = 0$  (see (37)), and  $\mu = \mu_c$  accepted above, and look at special points where the first and the second derivatives of the function  $E(y)$  vanish simultaneously. Recall that  $E(y)$  is defined in (30) via

$$E(y) = \ln \left( 1 + e^{y-p(\frac{1}{2}f-\mu)} \right) - \frac{y^2}{2p}. \quad (45)$$

Its first derivative  $E'(y)$  is given in (32). It becomes zero when  $px - y - yx = 0$ , and hence (cf. (41)),

$$y = p \frac{x}{1+x}. \quad (46)$$

The second derivative  $E''(y)$  from (35) vanishes when  $x^2 + (2-p)x + 1 = 0$ , and this quadratic equation has the solutions

$$x_{1,2}(p) = \frac{p}{2} - 1 \pm \sqrt{p \left( \frac{p}{4} - 1 \right)}. \quad (47)$$

When  $p < p_c = 4$ , there are no real solutions  $x_{1,2}$ , and  $E''(y)$  is always negative as it should be (see (35)). At  $p = p_c = 4$ , the first real solution appears,  $x_0 = 1$ . This special case has been studied in Section 7.1.

And now we are interested in the region  $p > 4$ , where we obtain two different solutions from (47). Vanishing of  $E''(y)$  at  $x = x_{1,2}(p)$  means that it happens when (here we recall the definitions (31))

$$e^{u(y)} = x_{1,2}(p), \quad \text{that is} \quad u(y) = \ln x_{1,2}(p), \quad \text{and thus,} \quad y + p\mu - \frac{1}{2}pf = \ln x_{1,2}(p). \quad (48)$$

Therefore,  $E'(y)$  and  $E''(y)$  vanish simultaneously when we combine the conditions (46) and (47) into

$$y = \tilde{y}_{1,2}(p) = p \frac{x_{1,2}(p)}{1+x_{1,2}(p)}, \quad (49)$$

which defines the coordinates  $\tilde{y}_1(p)$  and  $\tilde{y}_2(p)$  of new special points. Reporting (49) to the last equation in (48) leads us to the values of  $\mu$ , with which the present setting is possible, namely

$$\mu_{1,2} = \mu_{1,2}(p) = \frac{1}{2} f - \frac{x_{1,2}(p)}{1 + x_{1,2}(p)} + \frac{1}{p} \ln x_{1,2}(p). \quad (50)$$

For such  $\mu_1$  and  $\mu_2$  with any  $p > 4$ , we have  $E'(\tilde{y}_{1,2}) = E''(\tilde{y}_{1,2}) = 0$ , and the function  $E(y)$  has horizontal inflection points with  $E'''(\tilde{y}_{1,2}) > 0$  (see (37)).

### 7.3.1 An example calculation

Let us do an example by calculating the corresponding curves at  $p = 6$ . This is the same choice of the temperature  $p$  as in figures 3 a) and 3 b) in [4, p. 13]. At  $p = 6$ , we have  $x_{1,2} = 2 \pm \sqrt{3}$ , the coordinates of inflection points are  $\tilde{y}_{1,2} = 6 \frac{2 \pm \sqrt{3}}{3 \pm \sqrt{3}}$ , and the associated values of the chemical potential are

$$\mu_{1,2} = \frac{1}{2} f - \frac{2 \pm \sqrt{3}}{3 \pm \sqrt{3}} + \frac{1}{6} \ln(2 \pm \sqrt{3}). \quad (51)$$

The plots of corresponding functions  $E(y)$  with  $f = 10$  are given in Fig. 5.

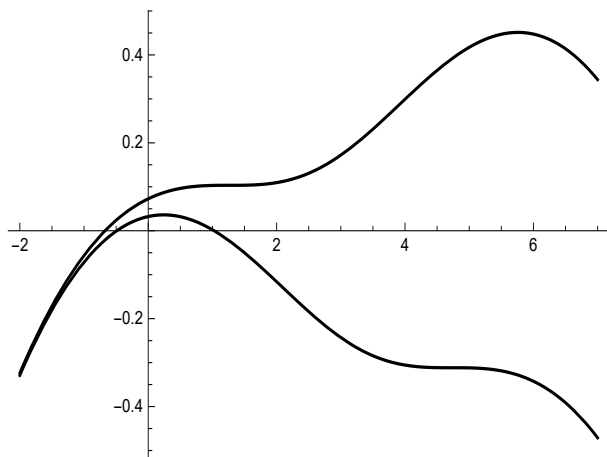


Fig. 5. Plots of the function  $E(y)$  from (30) with  $p = 6$ ,  $f = 10$ , and  $\mu_1 \simeq 4.43 < \mu_c$  (lower curve) and  $\mu_2 \simeq 4.57 > \mu_c$  (upper curve) given in (51) with plus and minus signs, respectively. The respective ordinates of inflection points are approximately  $-0.31$  and  $0.10$ .

Our Figure 5 combines, in fact, the plots of the same kind as in Figures 3 a) and 3 b) from [4, p. 13], into one. Indeed, they are very similar, though produced in a different setting involving the infinite sum over  $n$  instead of strongly truncated one in (29), and different physical parameters apart from  $p = 6$ .

### 7.3.2 A note on symmetry

A numerical check shows that the inequality

$$\mu_1 < \mu_c < \mu_2, \quad \mu_c = \frac{1}{2}(f - 1), \quad (52)$$

holds for chemical potentials  $\mu_1$  and  $\mu_2$  from (51) related to inflection points of  $E(y)$  at  $p = 6$ . This suggests that it could be a good idea to write these values as

$$\mu_1 = \mu_c + \frac{1}{2} - \frac{2 + \sqrt{3}}{3 + \sqrt{3}} + \frac{1}{6} \ln(2 + \sqrt{3}), \quad (53)$$

$$\mu_2 = \mu_c + \frac{1}{2} - \frac{2 + \sqrt{3}}{3 + \sqrt{3}} + \frac{1}{6} \ln(2 + \sqrt{3}). \quad (54)$$



Let us define *positive* deviations of  $\mu_1$  and  $\mu_2$  from the central value  $\mu_c$  via

$$\begin{aligned}\mu_c - \mu_1 &= -\frac{1}{2} + \frac{2 + \sqrt{3}}{3 + \sqrt{3}} - \frac{1}{6} \ln(2 + \sqrt{3}), \\ \mu_2 - \mu_c &= \frac{1}{2} - \frac{2 + \sqrt{3}}{3 + \sqrt{3}} + \frac{1}{6} \ln(2 + \sqrt{3}).\end{aligned}$$

A straightforward algebraic calculation shows that

$$\mu_c - \mu_1 = \mu_2 - \mu_c, \quad (55)$$

and hence,  $\mu_1 + \mu_2 = 2\mu_c = f - 1$ .

The values  $\mu_1$  and  $\mu_2$  from (51) are symmetric with respect to the critical value of chemical potential,  $\mu_c$  (see (34)). It would be of interest to check, whether the same symmetry property persists for generic values of  $\mu_k$  defined in (50).

### 7.3.3 Consequences of changes in $\mu$ at fixed temperature $p > p_c$

We finalize this section, dealing with the limit of large  $f$ , by showing the behavior of the function  $E(y)$  (see (30) and (45)) and its maxima at the fixed temperature,  $p = 6$ , and varying chemical potential  $\mu$ . The plots are given in Figure 6.

The first, blue line, corresponds to the lowest value of  $\mu$ ,  $\mu = 4 < \mu_c$ , while  $\mu = 4.5$ . The red line is drawn at  $\mu = \mu_c$ , the same line is shown in blue in Fig. 3. The two black lines with inflection points are the same as in Fig. 5. The magenta line corresponds to the largest value of  $\mu$ ,  $\mu = 4.64$ .

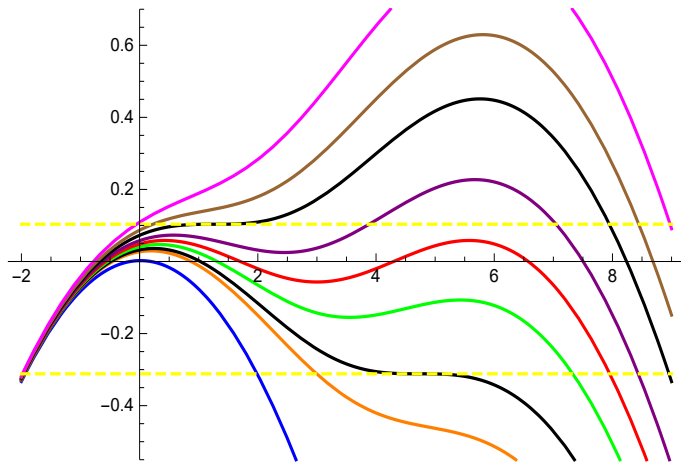


Fig. 6. Plots of the function  $E(y)$  from (30) with  $p = 6$ ,  $f = 10$ , and growing values of  $\mu$ : 4, 4.4,  $\mu_1$  from (51) and (53), 4.47,  $\mu_c = 4.5$ , 4.53,  $\mu_2$  from (51) and (54), 4.6, 4.64. The yellow dotted lines indicate the values of  $E(y)$  at the inflection points  $\tilde{y}_1$  and  $\tilde{y}_2$  given explicitly in the line preceding (51).

By the Laplace method, in the limit  $N \rightarrow \infty$ , the value of the integral over  $y$  in (30) is determined by the height of the global maximum attained by the function  $E(y)$ . In the region of  $\mu < \mu_c$ , such global maxima are situated roughly between  $y = 0$  and  $y = 1$ , see blue, orange, black, and green lines in the bottom of Fig. 6.

The red line at  $\mu = \mu_c$  signals a first-order phase transition. As far as  $\mu$  exceeds  $\mu_c$ , the global maximum jumps to a position between  $y = 5$  and 6. The "new" family of global maxima for  $\mu > \mu_c$  is shown by the purple, (second) black, brown, and magenta lines.

Finally, let us sketch the last consequence of  $\mu$  being not equal to  $\mu_c$ .

By analogy with (42), let us shift in (30) or (45) the integration variable  $y$  via  $y = s + pf/2 - p\mu$ . Thus we obtain

$$\hat{E}(\mu; s) = \ln(1 + e^s) - \frac{1}{2p} \left( s + p \left( \frac{1}{2} + \mu_c - \mu \right) \right)^2, \quad (56)$$

where we took into account the definition of  $\mu_c$  in (34). Expanding the last function in powers of  $s$  we obtain, similarly as in (44),

$$\hat{E}(\mu; s) = \ln 2 - \frac{p}{2} \left( \mu - \mu_c - \frac{1}{2} \right)^2 + (\mu - \mu_c) s + \frac{p-4}{8p} s^2 - \frac{s^4}{192} + O(s^6). \quad (57)$$

At  $\mu = \mu_c$ , the last expansion becomes an even function and reduces to the one in (44).

Similarly as at the end of Section 7.2, we could speculate here about certain equivalence of the present model with large enough repulsion between particles within a cell and such systems as lattice gas with non-zero chemical potential or Ising systems in the presence of an external ordering field.

## 8 Summary and outlook

On the physical side of the present paper, we propose the first analytical calculations for the Curie-Weiss cell model of fluid introduced in [4] and described in Section 2.1, for certain selected special cases.

First of all, explicit results for the simplest special cases of the ideal gas and the high-temperature limit are derived, in agreement with the well-known classical data (see Section 3).

Moreover, we have succeeded to show that the marginal case of equal attraction and repulsion interactions between the particles ( $J_1 = J_2$  in (2)) is meaningful and does not lead to any unphysical divergence of the integral representing the grand-canonical partition function of the system (see Sections 4 and 6). An explicit calculation in the asymptotic regime  $z \rightarrow +\infty$  showed a relation of this marginal equal-interaction case to the ideal-gas limit.

We have performed an extended analytical study of the strong-repulsion limit  $J_2 \gg J_1$  in Section 7 supported by numerous graphical representations and accompanied by discussions of related physical implications.

Explicit calculations performed in Sections 4 and 6 and their physical conclusions would be impossible without certain progress on the mathematical side.

Here, for the announced in the Abstract discrete Gauss-Poisson probability distribution function (A1), we have found the asymptotic behavior of its normalization  $R(r; z)$ , given by the infinite sum (A2), as  $z \rightarrow +\infty$ . In Section 5.1 we recorded the related results without proof, and a detailed exposition of the derivation is planned for the nearest future.

The asymptotic formulas found for the function  $\ln R(r; z)$  provide quite accurate approximations in a wide range of  $z$ , down to  $z \approx 3$ , which are illustrated in the left panels of Figures 1 and 2.

At large enough values of  $r$ , exceeding some threshold value  $r^*$ , the difference (24) between the function  $r \ln R(r; z)$  and its asymptotics becomes oscillatory. This interesting behavior is illustrated in the right-hand side of Figure 2. At this point we would like to notice two other instances where the periodic oscillatory behavior emerges in quite different situations, interesting from the mathematical point of view. These are [24, Sec. 4] and [25, p. 11, Fig. 4].

Certainly, this special kind of oscillatory behavior deserves a further investigation.

## Acknowledgements

We are grateful to our colleagues in the NRFU project, M.P. Kozlovskii, I.V. Pylyuk, and R.V. Romanik, for weekly enlightening and stimulating discussions. A careful reading of the draft

by R.V. Romanik and his suggestions are gratefully acknowledged. Special thanks of MAS are to M.P. Kozlovskii for his personal invitation to join the project.

The financial support by the National Research Foundation of Ukraine under the project No. 2023.03/0201 is gratefully acknowledged.

## References

- [1] S. M. Petrenko, O. L. Rebenko and M. V. Tertychnyi, *Quasicontinuous approximation in classical statistical mechanics*, *Ukr. Math. J.* **63** (2011) 425 – 442.
- [2] O. L. Rebenko, *Quasicontinuous approximation in classical statistical mechanics*, *Rev. Math. Phys.* **25** (2013) 1330006.
- [3] M. P. Kozlovskii, O. A. Dobush and R. V. Romanik, *Concerning a calculation of the grand partition function of a fluid model*, *Ukr. J. Phys.* **60** (2015) 805–822.
- [4] Yu. V. Kozitsky, M. P. Kozlovskii and O. A. Dobush, *A phase transition in a Curie-Weiss system with binary interactions*, *Condens. Matter Phys.* **23** (2020) 23502.
- [5] M. P. Kozlovskii and O. A. Dobush, *Phase behavior of a cell model with Curie-Weiss interaction*, *J. Mol. Liq.* **353** (2022) 118843.
- [6] O. A. Dobush, M. P. Kozlovskii, R. V. Romanik and I. V. Pylyuk, *Thermodynamic response functions in a cell fluid model*, [2409.09786](#).
- [7] J.-P. Hansen and I. R. McDonald, *Theory of Simple Liquids: with Applications to Soft Matter*. Academic Press, 4th ed., 2013.
- [8] Yu. Kozitsky and M. Kozlovskii, *A phase transition in a continuum particle system with binary Curie-Weiss interactions*, [1610.01845v1](#).
- [9] Yu. V. Kozitsky, M. P. Kozlovskii and O. A. Dobush, *Phase transitions in a continuum Curie-Weiss system: A quantitative analysis*, in *Modern Problems of Molecular Physics* (L. A. Bulavin and A. V. Chalyi, eds.), (Cham), pp. 229 – 251, Springer International Publishing, 2018. [DOI](#).
- [10] O. A. Dobush, M. P. Kozlovskii and R. V. Romanik, *Supercritical crossover lines in the cell fluid model*, [2410.23694](#).
- [11] D. Ruelle, *Superstable interactions in classical statistical mechanics*, *Commun. Math. Phys.* **18** (1970) 127 – 159.
- [12] T. L. Hill, *Statistical Mechanics*. McGraw-Hill, New York, 1956.
- [13] N. G. de Bruijn, *Asymptotic methods in analysis*. North-Holland Publishing Co., Amsterdam, 1958.
- [14] C. M. Bender and S. A. Orszag, *Advanced Mathematical Methods for Scientists and Engineers*. McGraw-Hill, New York, 1978.
- [15] P. Flajolet and R. Sedgewick, *Analytic Combinatorics*. Cambridge University Press, Cambridge, 2009, [10.1017/CBO9780511801655](#).

- [16] R. B. Paris, *The discrete analogue of Laplace's method*, *Comp. Math. Appl.* **61** (2011) 3024 – 3034.
- [17] E. T. Copson, *Asymptotic Expansions*. Cambridge University Press, Cambridge, 1965.
- [18] M. V. Fedoryuk, *Asymptotic methods in analysis*, in *Analysis I. Integral Representations and Asymptotic Methods* (R. V. Gamkrelidze, ed.), vol. 13 of *Encyclopedia of Mathematical Sciences*, pp. 83 – 191. Springer, 1989. DOI.
- [19] R. Wong, *Asymptotic Approximations of Integrals*. Academic Press, New York, 1989, [10.1016/C2013-0-07651-7](https://doi.org/10.1016/C2013-0-07651-7).
- [20] R. B. Paris, *Hadamard Expansions and Hyperasymptotic Evaluation*, vol. 141. Cambridge University Press, Cambridge et. al., 2011.
- [21] N. M. Temme, *Asymptotic Methods for Integrals*, vol. 6 of *Series in Analysis*. World Scientific, New Jersey et. al., 2015, [10.1142/9195](https://doi.org/10.1142/9195).
- [22] R. M. Corless, G. H. Gonnet, D. E. G. Hare, D. J. Jeffrey and D. E. Knuth, *On the Lambert W function*, *Adv. Comput. Math.* **5** (1996) 329 – 359.
- [23] Wolfram Research, Inc., *Mathematica, Version 12.3*. Champaign, Illinois, 2021.
- [24] R. Garrappa, S. Rogosin and F. Mainardi, *On a generalized three-parameter wright function of Le Roy type*, *Fract. Calc. Appl. Anal.* **20** (2017) 1196 – 1215.
- [25] M. A. Shpot, *A Ramanujan's hypergeometric transformation formula, its validity range and implications*, [2411.19608](https://doi.org/10.2411/19608).